Radiative forcing and albedo feedback from the northern hemisphere cryosphere between 1979 and 2008

M. G. Flanner[1]*, K. M. Shell[2], M. Barlage[3], D. K. Perovich[4], & M. A. Tschudi[5]

[1]*Department of Atmospheric, Oceanic and Space Sciences,*

University of Michigan, Ann Arbor MI, USA

[2]*College of Oceanic and Atmospheric Sciences, Oregon State University, Corvallis OR, USA*

[3]*National Center for Atmospheric Research, Boulder CO, USA*

[4]*Cold Regions Research and Engineering Laboratory, U.S. Army Engineer Research and Development Center, Hanover NH, USA*

[5]*Colorado Center for Astrodynamics Research, University of Colorado, Boulder CO, USA*

* Corresponding author. Contact: flanner@umich.edu

1 Extended Discussion

Potential sources of bias: Pre-1999 snow cover within an earlier version of our dataset[1] is reportedly overestimated in mountainous areas[2]. Here, we find large ΔCrRF over the Himalaya, Tien Shan, and Rocky Mountains, and negative ΔCrRF over the eastern Tibetan Plateau (Figure 2b). In a sensitivity study excluding snow changes over the Himalaya and Rockies, however, we find that northern hemisphere (NH) ΔCrRF$_{snow}$ is reduced by only 10%, indicating such biases would have a relatively small effect on our conclusions. The timing, however, of peak ΔCrRF$_{snow}$ within the ISCCP and APP-x kernels shifts from June to March, suggesting the seasonal cycle of ΔCrRF may be sensitive to mountain snow cover retrievals. Consistent with our analysis, previous work found that insolation-weighted snow cover changes during 1972–2006 peaked in June[2]. Unresolved mountain snow cover and glaciers cause low bias in our CrRF$_{snow}$ estimates, but have an unknown effect on ΔCrRF$_{snow}$.

Further uncertainty derives from the pole-centered void of sea-ice data, resulting from satellite orbit, which we fill with a nearest-neighbor algorithm. Excluding cryosphere change from this region reduces NH ΔCrRF$_{ice}$ by less than 2%, however, indicating this is a minor contribution to uncertainty. It is reasonable to expect that the void is mostly ice-covered during the time-series because the immediate perimeter of the void has high sea-ice fraction during most of the period.

A recent study determined that MODIS albedo retrievals (flagged lower quality) over Greenland are systematically biased low when solar zenith angle is large[3]. If such biases are systematic over snow, in general, our $\Delta\alpha_{snow}$ estimates may also be biased low, especially during local winter.

Because albedo biases at large solar zenith angle have smaller influence on energy balance biases, we do not expect this bias to have a large impact on our findings, but we note that it is a potential source of low bias in our CrRF estimates.

Finally, unresolved spectral variation in the radiative kernel technique may also introduce error. Snow and ice induce greater albedo contrast in the visible portion of the spectrum than in the near-infrared, whereas the radiative kernels are generated with spectrally-uniform surface albedo perturbations (but with spectrally-varying surface fluxes). Errors would arise in cases where the kernels exhibit different TOA attenuation of visible and near-infrared albedo anomalies and also have visible/near-infrared surface flux partitions that differ significantly from actual partitions in cryospheric regions. In a sensitivity study, we compared CrRF estimates derived from solar broadband quantities (MODIS albedo contrast and CAM3 radiative kernel) with CrRF derived from the same products partitioned into visible and and near-infrared components. This study found differences in ΔCrRF only on the order of 5%.

Comparison with previous studies: An earlier study[4] combined snow cover maps with remotely-sensed TOA flux variability to quantify mean 1973–1992 all-sky shortwave CrRF of $-9.2\,\mathrm{W\,m^{-2}}$ over snow-affected regions, or $-1.9\,\mathrm{W\,m^{-2}}$ averaged over the northern hemisphere (NH). Using very different techniques, we calculate mean NH land-based CrRF of $-2.0\,\mathrm{W\,m^{-2}}$ for 1979–2008, offering encouraging agreement in the absolute radiative effect of land-based snow cover.

Recent remote sensing analyses of the April–May seasonal change in NH land surface albedo with temperature $(d\alpha/dT)$[5–7] decomposed this term into contributions from changes in snow cover

and changes in albedo of snow-covered surfaces[6,7]. These studies found[7] that the former and latter components are, respectively, -0.54 ± 0.07 and $-0.52 \pm 0.04\,\%\,K^{-1}$ averaged over land north of 30°N during 1982–1999. From seasonal change in CrRF, we estimate $d\alpha/dT$ of $-0.61 \pm 0.07\,\%\,K^{-1}$ over the same spatial domain. The standard deviation represents the interannual variability in April–May feedback during 1979–2008. Our estimate represents the contribution to altered surface albedo of changes in snow cover between April and May, but with different albedo contrast and insolation distributions applied in April and May, following our definition of CrRF. Fixing TOA insolation at April levels, as done previously[5], yields a feedback estimate of $-0.74 \pm 0.07\,\%\,K^{-1}$. Fixing snow-free albedo, snow-covered albedo, and TOA insolation at April values, to isolate a contribution from altered snow cover alone, yields an estimate of $-0.60 \pm 0.07\,\%\,K^{-1}$, within statistical uncertainty of the previous estimates. The recent study[7] found a surprisingly large contribution of snow-covered albedo change (the "metamorphism" component) to bulk albedo feedback. Because the snow cover product we apply in this study is binary, our ability to resolve the metamorphism contribution is limited. However, if we constrain our analysis to grid-cells that are only snow-covered in both April and May, and maintain constant April snow-free albedo between each month, we estimate an April–May metamorphism feedback component of only $-0.08 \pm 0.03\,\%\,K^{-1}$. Analysis with resolved snow cover fraction and resolved albedo of that snow-covered portion would yield a more accurate estimate of this component[7].

Global cryosphere feedback: We constrained our study to the northern hemisphere (NH) for several reasons, including: 1) The area covered by seasonal snow and sea-ice is much greater in the NH than southern hemisphere (SH), 2) The snow cover product[1] that we applied only covers the

NH, and we are unaware of SH land snow cover products extending back to 1979, and 3) climate changes during the last 30 years have been larger in the NH than in the SH[8]. We speculate here, briefly, on possible global cryosphere feedback. As with Greenland, changes in Antarctic land ice cover would not contribute much to 30-year change in CrRF. SH sea-ice cover actually increased at a rate of 1 % decade^{-1} during 1979–2006[9]. As emphasized in our main discussion, the seasonal dependence of these trends is critically important for the radiative effect, and this study did find increases in SH sea-ice during spring and summer, though they were not statistically significant. Seasonal land snow cover in the SH is quite small. Global surface warming during 1979–2008 was smaller than NH warming. Using the same linear analysis we applied for NH trends, we find 1979–2008 global warming of 0.47°C in both the NASA GISS and HadCRUT3v datasets. If, for the sake of argument, we assume that changes in the southern hemisphere cryosphere contributed negligibly to global changes in CrRF, the global cryosphere albedo feedback (derived from central NH ΔCrRF and global warming) would be $0.48\,\mathrm{W\,m^{-2}\,K^{-1}}$. Because of slight increases in SH sea-ice extent, the actual feedback may be slightly smaller, though decreases in SH land snow could have offset the sea-ice change. Clearly, a more detailed analysis of southern hemisphere cryosphere feedback is needed.

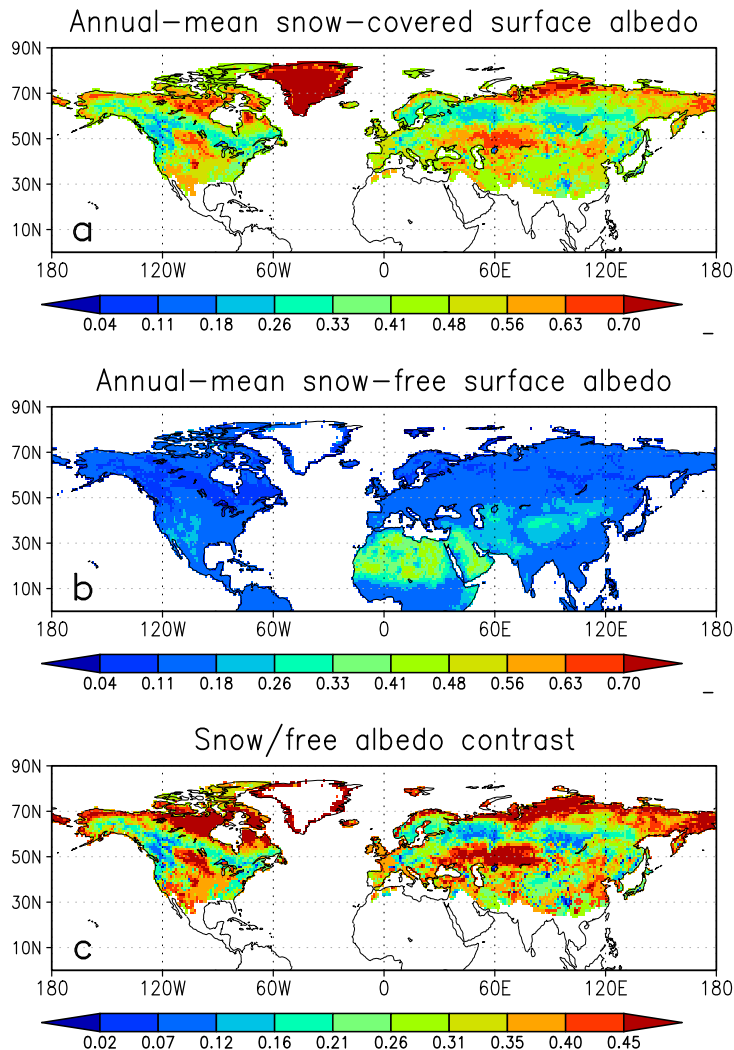## 2   Supplementary figures and tables

Figure S1 Annual-mean albedo (insolation-weighted) of surfaces defined as snow-covered within the NOAA/Rutgers product (a), of snow-free surfaces from MODIS (b), and their difference (c). Note the different scale applied to (c). Snow-covered albedo is filled in decreasing priority with MODIS product MCD43C3 (monthly-resolved, then annual-mean), APP-x data, and MODIS land-class means (Table S1). Snow-free albedo is derived entirely from MODIS. Monthly-varying data shown in (c) define the albedo contrast ($\Delta\alpha_{\mathrm{snow}}$) applied to calculate central estimates of cryosphere radiative forcing (CrRF).
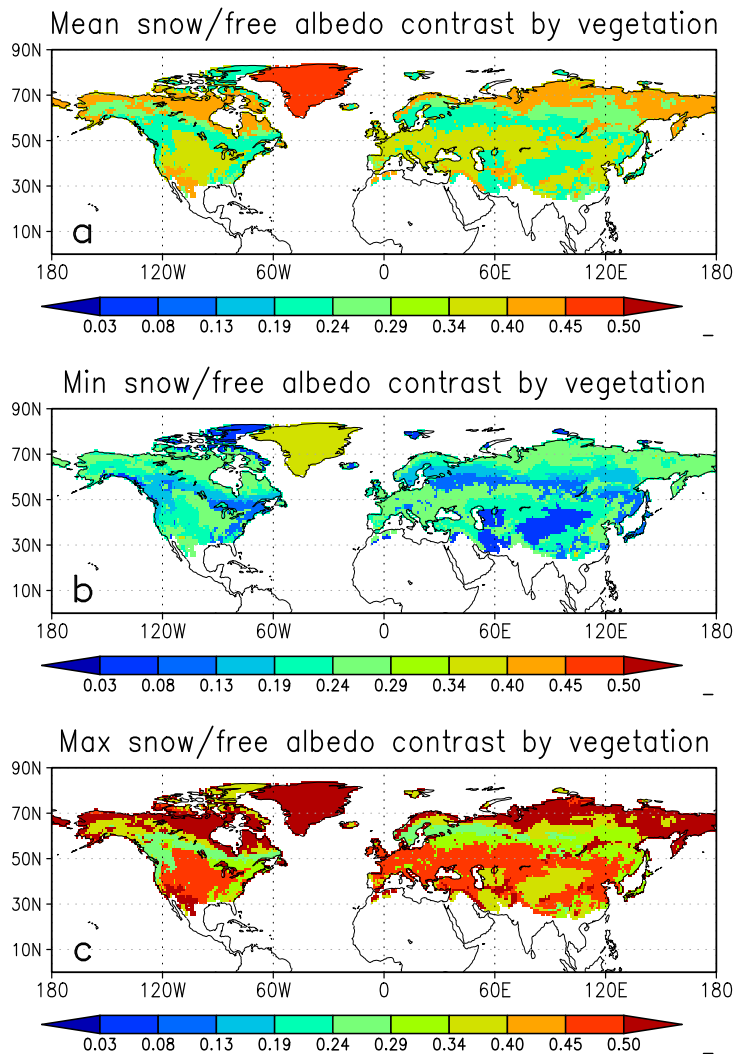
Figure S2 Mean (a), minimum (b), and maximum (c) insolation-weighted annual-mean albedo contrast between snow-covered and snow-free surface, using only MODIS land-class mean data, shown in Table S1. Minimum (maximum) datasets are determined by subtracting (adding) the combined variances of snow-covered and snow-free albedo from MODIS (Table S1) and compose the minimum (maximum) $\Delta\alpha_{\mathrm{snow}}$ data used to bound CrRF (Tables 1 and 2).
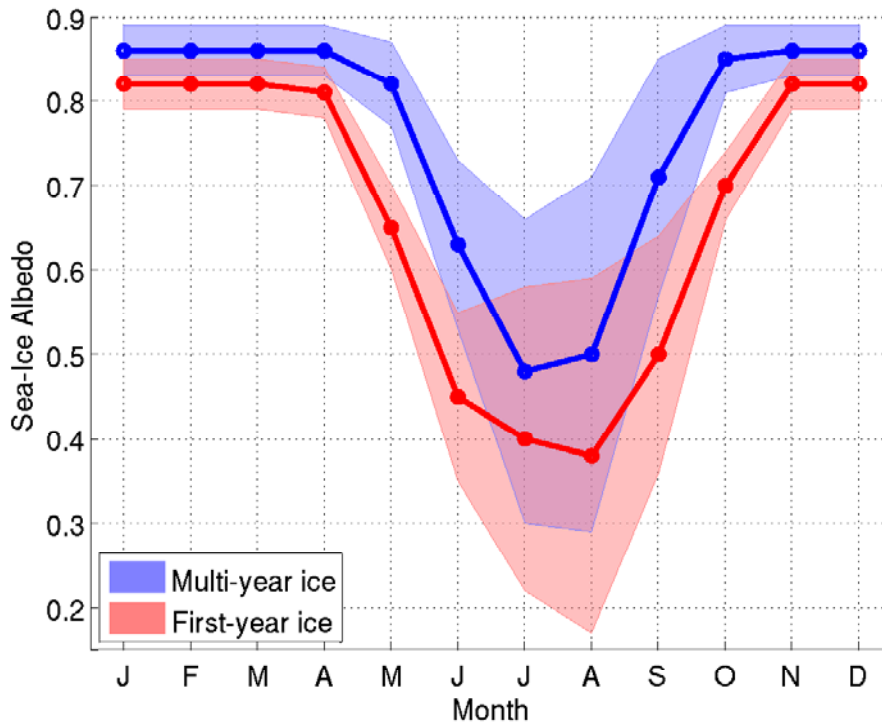
Figure S3 Seasonal cycle of multi-year and first-year sea-ice albedo, with shading indicating the ranges applied for minimum and maximum $\Delta\alpha_{\mathrm{ice}}$ products. Multi-year ice albedo data are from published field measurements[10], and first-year ice albedo are from unpublished field measurements and remote sensing data[11,12] (Methods).
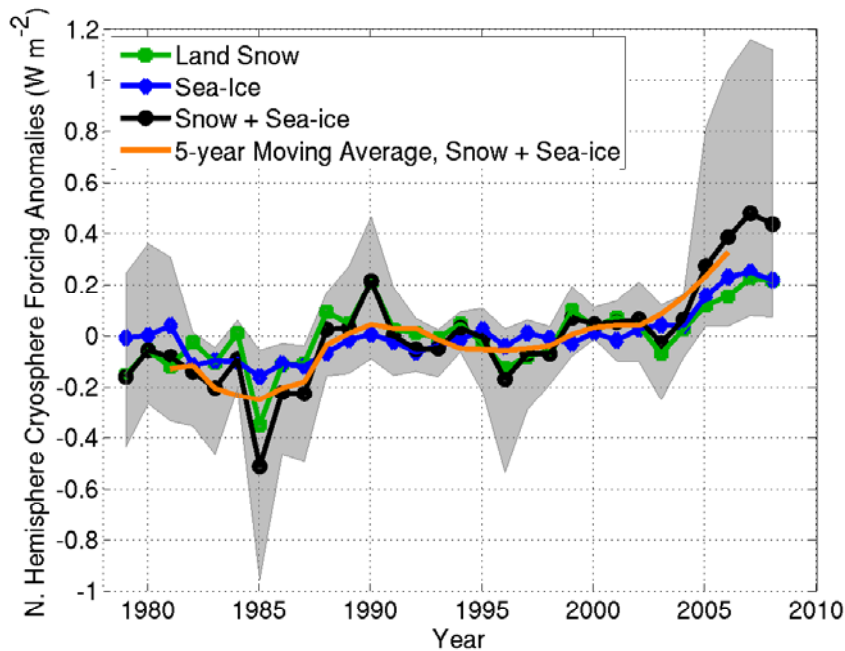
Figure S4 1979–2008 timeseries of cryosphere radiative forcing (CrRF) anomalies, relative to 1979–2008 means, from land-based snow, sea-ice, and the combination of both components. Each line depicts the mean anomalies of the 12 all-sky scenarios of albedo contrast and $\partial F/\partial \alpha$ listed in Tables 1 and 2, and shading indicates the full range of anomalies for the snow+sea-ice forcing from all 12 cases. The 5-year moving average of snow+sea-ice forcing anomaly is shown in orange.
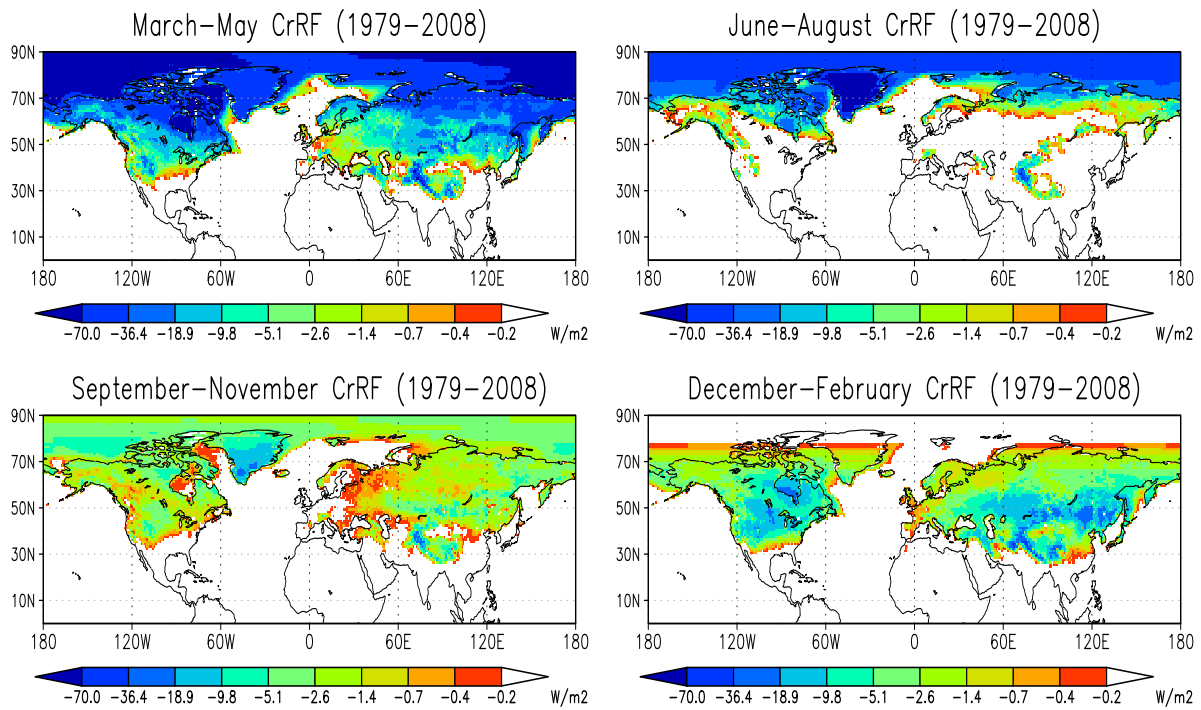
Figure S5   Seasonal components of cryosphere radiative forcing (CrRF), averaged over 1979–2008, depicted on a logarithmic scale. Annual-mean CrRF is shown in Figure 2a.
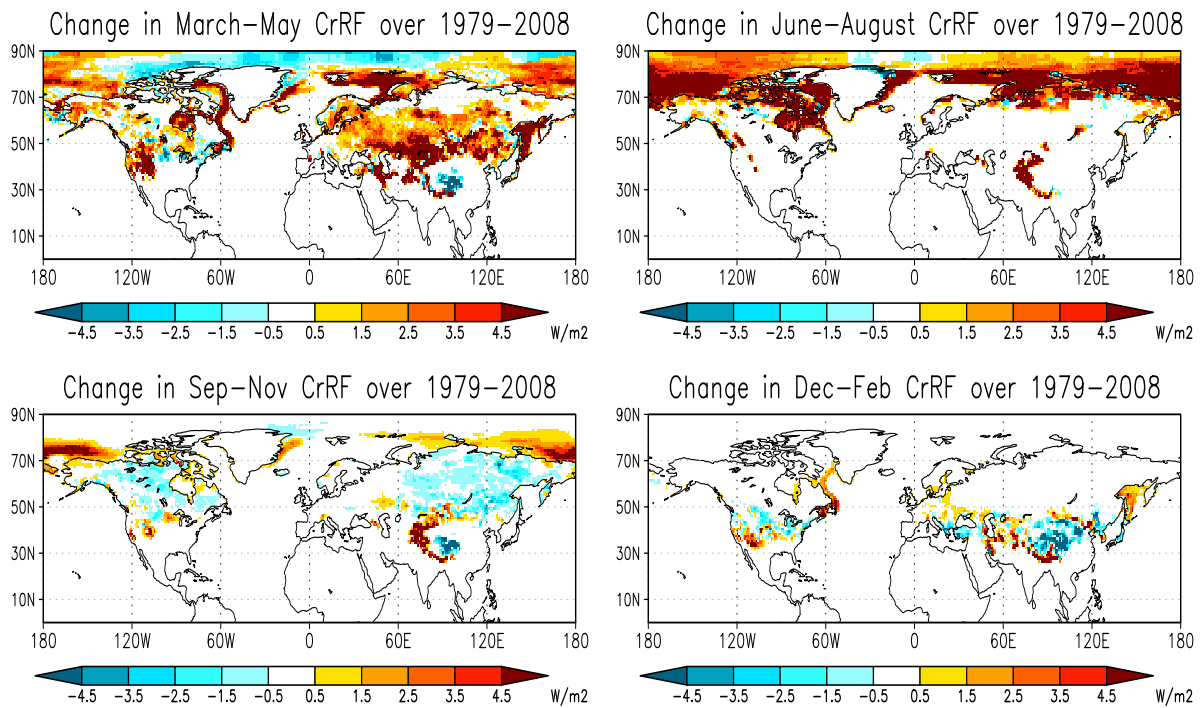
Figure S6   Seasonal components of the change in cryosphere radiative forcing (CrRF) from 1979 to 2008, determined from linear trend analysis. Annual-mean change in CrRF is shown in Figure 2b.

Table S1 MODIS Mean (μ) and Standard Deviation (σ) of Snow-Covered and

Snow-Free Surface Albedo by Land Class[a]

UMD Land Class	Snow-covered albedo[b]		Snow-free albedo	
	μ	σ	μ	σ
Evergreen needleleaf forest	0.31	0.07	0.10	0.02
Evergreen broadleaf forest	–	–	0.14	0.01
Deciduous needleleaf forest	0.36	0.06	0.12	0.01
Deciduous broadleaf forest	0.35	0.08	0.14	0.02
Mixed forest	0.34	0.09	0.12	0.02
Closed shrublands	0.59	0.06	0.15	0.02
Open shrublands	0.60	0.12	0.19	0.05
Woody savannas	0.42	0.08	0.14	0.02
Savannas	0.49	0.09	0.16	0.02
Grasslands	0.55	0.13	0.19	0.04
Croplands	0.55	0.10	0.16	0.03
Urban and built-up	–	–	0.12	0.02
Barren or sparsely vegetated	0.48	0.14	0.26[c]	0.07
Greenland	0.76	0.07	0.26[d]	0.07

[a] Mean values are weighted by insolation and gridcell area

[b] Snow-covered albedo statistics are determined from binary snow-covered gridcells

defined by the NOAA/Rutgers product, which has a threshold of 50% for snow cover.

[c] Averaged over land north of $30°$N

[d] Measured ground albedo at the northern edge of the Greenland Ice Sheet is 0.17[13]

Table S2 PCMDI AR4 model simulations used in the analysis of 1981–2010 albedo feedback, where simulations from 20th century (20C3M) and 21st century (SRES A1B) scenarios were used.

Model	Modeling center
BCCR BCM2	Bjerknes Center for Climate Research
CCCMA CGCM3 (T47)	Canadian Centre for Climate Modelling and Analysis
CCCMA CGCM3 (T63)	Canadian Centre for Climate Modelling and Analysis
CNRM CM3	Center National de Recherches Meteorologiques
GFDL CM2.0	Geophysical Fluid Dynamics Laboratory
GFDL CM2.1	Geophysical Fluid Dynamics Laboratory
GISS AOM	Goddard Institute for Space Studies
GISS EH	Goddard Institute for Space Studies
IAP FGOALS1	Institute for Atmospheric Physics
INM CM3	Institute for Numerical Mathematics
MIROC(hires)	Center for Climate System Research
MIROC(medres)	Center for Climate System Research
MIUB ECHO	Meteorological Institute University of Bonn
MPI ECHAM5	Max Planck Institute for Meteorology
MRI CGCM2	Meteorological Research Institute
NCAR CCSM3	National Center for Atmospheric Research
NCAR PCM1	National Center for Atmospheric Research
UKMO HadCM3	Met Office's Hadley Centre for Climate Prediction

3   References

1. Robinson, D. A. & Frei, A. Seasonal variability of northern hemisphere snow extent using visible satellite data. *Professional Geographer* **51**, 307–314 (2000).

2. Déry, S. J. & Brown, R. D. Recent Northern Hemisphere snow cover extent trends and implications for the snow-albedo-feedback. *Geophys. Res. Lett.* **34**, L22504 (2007).

3. Wang, X. & Zender, C. Constraining MODIS snow albedo at large solar zenith angles: Implications for the surface energy budget in Greenland. *J. Geophys. Res.,* **115**, F04015 (2010).

4. Groisman, P. Y., Karl, T. R. & Knight, R. W. Observed impact of snow cover on the heat balance and the rise of continental spring temperatures. *Science* **263**, 198–200 (1994).

5. Hall, A. & Qu, X. Using the current seasonal cycle to constrain snow albedo feedback in future climate change. *Geophys. Res. Lett.* **33**, L03502 (2006).

6. Qu, X. & Hall, A. What controls the strength of snow-albedo feedback? *J. Climate* **20**, 3971–3981 (2007).

7. Fernandes, R. *et al.* Controls on northern hemisphere snow albedo feedback quantified using satellite earth observations. *Geophys. Res. Lett.* **36**, L21702 (2009).

8. Trenberth, K. E. *et al.* Observations: Surface and atmospheric climate change. In *Climate Change 2007: The Physical Science Basis* (Cambridge University Press, 2007).

9. Cavalieri, D. J. & Parkinson, C. L. Antarctic sea ice variability and trends, 1979–2006. *J. Geophys. Res.* **113**, C07004 (2008).

10. Perovich, D. K., Grenfell, T. C., Light, B. & Hobbs, P. V. Seasonal evolution of the albedo of multiyear Arctic sea ice. *J. Geophys. Res.* **107** (2002).

11. Wang, X. & Key, J. R. Arctic surface, cloud, and radiation properties based on the AVHRR Polar Pathfinder Dataset. Part I: Spatial and temporal characteristics. *J. Climate* **18**, 2558–2574 (2005).

12. Tschudi, M. A., Fowler, C., Maslanik, J. A. & Stroeve, J. Tracking the movement and changing surface characteristics of Arctic sea ice. *IEEE J. Selected Topics in Earth Obs. and Rem. Sens.* (2010).

13. Bøggild, C. E., Brandt, R. E., Brown, K. J. & Warren, S. G. The ablation zone in northeast Greenland: ice types, albedos and impurities. *J. Glaciol.* **56**, 101–113 (2010).